

**Editors:**

**Jianchun Li, Xiaozhao Li, Minghe Ju,  
Fengqiang Gong, and Yingxin Zhou**



# **ROCK DYNAMICS**

**PROGRESS AND PROSPECT**

**Volume 2**



**CRC Press**  
Taylor & Francis Group

## ROCK DYNAMICS: PROGRESS AND PROSPECT VOLUME 2

**Rock Dynamics: Progress and Prospect** contains 152 scientific and technical papers presented at the Fourth International Conference on Rock Dynamics and Applications (RocDyn-4, Xuzhou, China, 17-19 August 2022). The two-volume set has 7 sections. Volume 1 includes the first four sections with 6 keynotes and 5 young scholar plenary session papers, and contributions on analysis and theoretical development, and experimental testing and techniques. Volume 2 contains the remaining three sections with 74 papers on numerical modelling and methods, seismic and earthquake engineering, and rock excavation and engineering.

**Rock Dynamics: Progress and Prospect** will serve as a reference on developments in rock dynamics scientific research and on rock dynamics engineering applications. The previous volumes in this series (RocDyn-1, RocDyn-2, and RocDyn-3) are also available via CRC Press.

PROCEEDINGS OF THE FOURTH INTERNATIONAL CONFERENCE ON ROCK DYNAMICS  
AND APPLICATIONS (ROCDYN-4), 17-19 AUGUST 2022, XUZHOU, CHINA

# Rock Dynamics: Progress and Prospect

Volume 2

*Editors*

Jianchun Li

*Southeast University, Nanjing, China*

Xiaozhao Li

*China University of Mining and Technology, Xuzhou, China*

Minghe Ju

*China University of Mining and Technology, Xuzhou, China*

Fengqiang Gong

*Southeast University, Nanjing, China*

Yingxin Zhou

*Deeptek Pty Ltd, Monash, Victoria, Australia*



**CRC Press**

Taylor & Francis Group

Boca Raton London New York

---

CRC Press is an imprint of the  
Taylor & Francis Group, an **informa** business

A BALKEMA BOOK

Designed covered image: Triaxial Hopkinson Bar System

First published 2023  
by CRC Press/Balkema  
4 Park Square, Milton Park, Abingdon, Oxon, OX14 4RN  
e-mail: enquiries@taylorandfrancis.com  
www.routledge.com – www.taylorandfrancis.com

*CRC Press/Balkema is an imprint of the Taylor & Francis Group, an informa business*

© 2023 selection and editorial matter, Jianchun Li, Xiaozhao Li, Minghe Ju, Fengqiang Gong & Yingxin Zhou; individual chapters, the contributors

The right of Jianchun Li, Xiaozhao Li, Minghe Ju, Fengqiang Gong & Yingxin Zhou to be identified as the authors of the editorial material, and of the authors for their individual chapters, has been asserted in accordance with sections 77 and 78 of the Copyright, Designs and Patents Act 1988.

All rights reserved. No part of this book may be reprinted or reproduced or utilised in any form or by any electronic, mechanical, or other means, now known or hereafter invented, including photocopying and recording, or in any information storage or retrieval system, without permission in writing from the publishers.

Although all care is taken to ensure integrity and the quality of this publication and the information herein, no responsibility is assumed by the publishers nor the author for any damage to the property or persons as a result of operation or use of this publication and/or the information contained herein.

*Library of Congress Cataloging-in-Publication Data*

A catalog record has been requested for this book

SET

ISBN: 978-1-032-41659-5 (hbk)

ISBN: 978-1-032-41662-5 (pbk)

Volume 1:

ISBN: 978-1-032-41663-2 (hbk)

ISBN: 978-1-032-41667-0 (pbk)

ISBN: 978-1-003-35914-2 (ebk)

DOI: 10.1201/9781003359142

Volume 2:

ISBN: 978-1-032-41664-9 (hbk)

ISBN: 978-1-032-41665-6 (pbk)

ISBN: 978-1-003-35915-9 (ebk)

DOI: 10.1201/9781003359159

An artificial neural network-based model for blast-induced ground vibration prediction in urban area	229
<i>N. Ogunsola, J. Pureun, S. Cho &amp; Y. Kim</i>	
Application of three-dimensional laser point cloud technology to river management	235
<i>N. Akiyama, S. Nishiyama &amp; J. Song</i>	
Automatic extraction of rockfall source based on terrain analysis map using support vector machine	240
<i>N. Sakamoto, K. Sakita, S. Nishiyama, T. Kikuchi, J. Song &amp; Y. Ohnishi</i>	
Changes in reservoir stress from faults and productions	246
<i>Y. Li, Y. Lu, D. Xu, H. Hao, Q. Na, W. Zhou &amp; C. Xu</i>	
Consideration of countermeasures using rockfall simulation by discontinuous deformation analysis	252
<i>H. Kitauchi, S. Nishiyama &amp; J. Song</i>	
Developing a real-time safety information model for large-scale underground cavern group	258
<i>A. Hu, M. Wu, S. Zhou, R. Zhao &amp; X. Liu</i>	
Development of particle discontinuous deformation analysis method and its application in rock blasting	263
<i>L. Huang, C. Li, J. Chen, J. Ma &amp; W. Chen</i>	
Displacement and damage characteristics of underground fortification under blast loading	268
<i>Q. Lin, S. Li, C. Feng, Y. Gan, J. Yuan, W. Jiao, Y. Zhang &amp; H. Jiang</i>	
Dynamic behaviors of the stressed circular tunnel under cylindrical <i>P</i> wave	274
<i>H. Zhao, X. Li, M. Tao, H. Gu, R. Zhao &amp; Z. Hong</i>	
Dynamic stability assessment of a wedge-like huge rock block at Itoman Rotary, Okinawa, Japan	280
<i>T. Ito, Ö. Aydan, N. Tokashiki, H. Inoue &amp; Y. Higa</i>	
Dynamic support design in very deep hard rock mines: A state-of-the-art review	286
<i>S. Shnorhokian &amp; G. Raju</i>	
Experimental investigations on rock damage extent induced by three blast techniques	291
<i>X. Xia, J. Zhang, H. Li, Y. Liu, C. Yu &amp; B. Liu</i>	
Investigation of coal burst mechanism based on three cases	296
<i>N. Zhang, J. Jiang, Z. Deng, S. Zhao, G. Zhang, Y. Zhao &amp; Z.-X. Zhang</i>	
Non-deterministic dynamics of mining-induced ground oscillations	302
<i>S. Kostić &amp; N. Vasović</i>	
Numerical analysis of vibration induced by bench blasting with different blasting parameters of rock tunnel excavation	307
<i>Y. Liang, X. Li &amp; J. Li</i>	
Numerical and experimental study on the dynamic penetration performance of TBM cutterhead using a FEA-SPH coupling method	313
<i>Q. Geng, M. Ma, L. Renqian, J. Hui, M. Ye, X. Wang &amp; Z. Zhang</i>	

## Preface

The international conference series on rock dynamics is usually held every 2-3 years. Following the third conference in 2018, the Fourth International Conference on Rock Dynamics and Applications (RocDyn-4) was originally planned in 2021. Affected by the outbreak of Covid-19, RocDyn-4 was delayed to 2022, and for the first time, is held in a hybrid format of on-site and virtual attendance.

With increasing activities of the rock dynamics community, RocDyn-4 has received overwhelming responses. The conference has received over 200 abstracts and finally accepted 152 papers to be included in the proceedings. The topics cover from theories, testing and modelling to engineering, reflecting the progress and the prospect of rock dynamics as suggested by the title of the conference.

The two volumes of the proceedings include 6 keynote papers, 5 selected papers of young scholar plenary session, and 5 sections of technical papers, namely, (i) analysis and theoretical development, (ii) experimental testing and techniques, (iii) numerical modelling and methods, (iv) seismicity and earthquake engineering, and (v) rock excavation and engineering. We are delighted to see many papers span over 2 or even 3 sections, indicating the integration among research methodologies and the integration between research and engineering.

Certainly, the progress of rock dynamics and applications is not just in the numbers but can also be seen in the advances in various aspects of rock dynamics. It is not possible to list all new developments but the multi-axial and the electro-magnetic Hopkinson bars, and the role of rock dynamics in energy extraction and geological carbon sequestration, represent some good examples. While progress has been made, challenges remain in the study of rock dynamics, not the least because of the “4<sup>th</sup> dimension” of time. Much work remains to be done. We hope the proceedings can provide a good reference to researchers and engineers, and we invite the readers to read and discover more in the 2 proceedings volumes.

RocDyn-4 is a specialised symposium of the International Society for Rock Mechanics and Rock Engineering (ISRM). The conference is organised by China University of Mining and Technology in Xuzhou and Southeast University in Nanjing, in association with ISRM Commission on Rock Dynamics. It is supported by Chinese Society for Rock Mechanics and Engineering, State Key Laboratory for Geomechanics and Deep Underground Engineering, Yunlong Lake Laboratory of Deep Underground Science and Engineering, and an International Advisory Committee overseeing the RocDyn conference series.

The editors would like to thank all the authors for their contributions and members of the Advisory Committee and the Organising Committee for reviewing the papers to ensure a high-quality conference. The proceedings are prepared by the editors with editorial support of Haiying Bian of China University of Mining and Technology (Beijing) and the CRC publishing team including Léon Bijnsdorp, Kaustav Ghosh, Richard Gundel and Renate Bonte.

Jian Zhao and Yingxin Zhou

August 2022

# Non-deterministic dynamics of mining-induced ground oscillations

Srđan Kostić\*

Jaroslav Černi Water Institute, Belgrade, Serbia

Nebojša Vasović

Faculty of Mining and Geology, University of Belgrade, Belgrade, Serbia

**ABSTRACT:** Recordings of ground acceleration induced by M2 seismic event triggered by deep mining are analyzed, in order to confirm the stochastic nature of the process. Three components of ground acceleration were examined: north-south, east-west and vertical. Surrogate data testing was conducted by testing the three hypotheses: the observed data are independent random numbers drawn from some fixed but unknown distribution, the recordings originate from a stationary linear stochastic process with Gaussian inputs and the recordings originated from a stationary Gaussian linear process that has been distorted by a monotonic, instantaneous, time-independent nonlinear function. Results of surrogate data testing indicate that ground acceleration triggered by deep mining belongs to a group of nonlinear systems and stochastic processes with Gaussian distribution of stochastic part. Analysis was conducted by embedding the recorded time series, for each direction, into appropriate embedding space using mutual information method (embedding delay) and false nearest neighbour technique (embedding dimension). Mutual information method resulted in the values of embedding delay of  $\tau = 29$ ,  $\tau = 18$  and  $\tau = 12$ , for each direction, while the false nearest neighbour method indicated that the percentage of false nearest neighbour increases with the increase of embedding dimension, confirming the absence of determinism in the recorded ground acceleration time series. Recorded series were further examined by invoking stationarity and deterministic test, including the calculation of maximal Lyapunov exponent. Deterministic factor  $\kappa < 1$ , relatively large cross-prediction error and a low value of maximal Lyapunov exponent confirm the stochasticity of the mining-induced ground acceleration. This is the first time that recordings of mining-induced seismic events are examined using the nonlinear time series analysis. Moreover, results obtained for the first time emphasize the need of stochastic approach in modelling the mining-induced ground oscillations.

## 1 INTRODUCTION

Research in the field of mining-generated earthquakes is mainly based on the assessment of hazards and risks of their impact on the excavation process itself, the progress of mining works, cost-effectiveness of exploitation, as well as applied mechanization, surface mining facilities and manpower. The first connection between nonlinear dynamics and chaos and mining-induced earthquakes is given by Morrison et al. (1993), where the authors, by the method of discrete elements, study the phenomenon of motion along faults (and thus earthquakes) depending on the distance from the excavation point. The results of their research point to the following conclusions: that the distribution of earthquakes (movements along faults) has unique (fractal) properties, and that the deterministic model in the case of earthquakes is acceptable only to a certain extent, i.e. that model improvement is possible if we start from the assumption that earthquake nucleation process represents

a “chaotic” system. Kortas (2005) investigated the seismograms of 5 major earthquakes recorded in Poland and South Africa. Two were registered in the Legnica-Glogow copper basin (in the Polkowice-Sieroszowice and Rudna mines), two in the Upper Silesian coal basin (in the Katowice and Vujek mines), while the fifth seismogram represents registered soil oscillations during an earthquake in a gold mine in South Africa. The research included the distribution of registered energy, registration time, epicenter coordinates and earthquake hypocenters. Using the Grasberger-Procaccia algorithm for determining the size of the fractal dimension, Kortas pointed out that the distribution of occurrence time, energy and epicenter coordinates has the property of multifractals (0.69-1.60 for copper mines, 0.62-2.56 for coal mines and 0.87-2.07 for a gold mine in South Africa). Also, Kortas calculated the value of the maximum Lyapunov exponent, whereby in 4 of the 20 cases studied the maximum Lyapunov exponent had a positive value, indicating high-dimensional

\*Corresponding author: srdjan.kostic@jcerni.rs

deterministic chaotic behavior of the system. On the other hand, Huang et al. (2010) investigated the model of two spring-loaded blocks, in order to simulate mining-generated earthquakes, and determined deterministic chaotic behavior, which indicates that the dynamics of mining-generated earthquake models is deterministic.

In present paper, we analyze recorded time series of ground acceleration due to mine-induced seismic event at Rudna copper mine in western Poland (Zembaty 2004). The analysis is performed numerically, in two phases: first, linearity testing is performed by surrogate data analysis, and then the dynamics of the observed time series is examined using the theory of scalar time series development in a certain time interval, proposed in Takens (1981).

## 2 DESCRIPTION OF THE CASE STUDY

The Rudna mine is located in western Poland, near the town of Polkowice, 350km southwest of Warsaw. It is one of the largest copper and silver mines in Poland, whose reserves are estimated at about 513 million tons of ore, with 1.78% copper and 42g/t of silver. It started operating in 1969. The ore is mined in three mining fields: Centralna Rudna (I), Zapadna Rudna (II) and Severna Rudna (III). In terms of geological structure, the southern border of the Lubin-Siroshovie region, to which the Rudna mine also belongs, is tectonic, represented by the deep Odra fault, as part of the wider Hamburg-Krakov tectonic zone. The Odra fault zone separates the Lubin-Siroshovica region from the For-Sudeten block of Proterozoic age (Oszczepalski 1989). The ore is excavated at depths of 600-1000 m, practically below the entire city and surrounding villages, in 13 pits, and that is classic, leaving protective pillars during excavation. Having in mind the complex tectonic structure of this terrain, with the existence of the deep fault zone Odra, which extends in the immediate vicinity of the ore body, any change in stress state also causes unstable balance along the fault, which causes earthquakes of different strengths. For that reason, the observation network of seismological stations was set up in a diameter of 6-8 km inside and outside the city. All instruments are set to record earthquakes with maximum acceleration (PGA) over  $10\text{cm/s}^2$ . A total of 32 vertical seismometers of the Vilmor MK-II and MK-III type were installed, with a frequency range of 0.5-150Hz and a dynamic range of 70dB. Regarding the earthquakes that occurred, based on the local earthquake catalog, in the period from January 1, 1980. until 03.03.2002 a total of 15573 earthquakes were registered, with a maximum local magnitude of  $M_L = 4.2$  (Kwiatk 2004).

## 3 APPLIED METHODOLOGY

Recorded ground acceleration is examined by the means of nonlinear time series analysis. We firstly conduct the surrogate data testing, by assuming that:

(1) the observed data are independent random numbers drawn from some fixed but unknown distribution; (2) the recordings originate from a stationary linear stochastic process with Gaussian inputs and (3) the recordings originated from a stationary Gaussian linear process that has been distorted by a monotonic, instantaneous, time-independent nonlinear function (Perc et al. 2008). For this purpose, we generated 20 surrogates and then, in order to compare the original data and generated surrogates, we calculated the zeroth-order prediction error  $\epsilon$ . If this error for the original dataset ( $\epsilon_0$ ) is smaller in comparison to the calculated error for surrogate data ( $\epsilon$ ), then a null hypothesis can be rejected. Usually, more than one wrong result out of 20 is not considered acceptable. The next step within this analysis was to embed the observed scalar series into the appropriate phase space using the Takens procedure (1981). The optimal embedding delay is calculated using average mutual information method, while the minimum embedding dimension is examined by the method of false nearest neighbors. Once the time series is embedded in the phase space, we applied stationarity test and a determinism test. Stationarity tests is based on cross-prediction error statistics and serves to confirm whether the examined data set originates from non-stationary process. The idea is to split the time series into several short non-overlapping segments and then use a particular data segment to make predictions in another data segment. This task then has to be repeated for all possible combinations. Determinism test is based on the assumption that if a time series originates from a deterministic process, it can be described by a set of the first-order ordinary differential equations, whose vector field consist solely of vectors that have unit length. In other words, if the system is deterministic, the average length of all directional vectors  $\kappa$  will be 1, while for a completely random system,  $\kappa \approx 0$ . As the final step, we calculated the value of maximum Lyapunov exponent.

## 4 RESULTS

The analysis of the ground acceleration was performed on the example of the mine-induced earthquake registered on February 2nd, 2001, at the station "3 Maja". The maximum registered ground acceleration (PGA) was  $51.6\text{ cm/s}^2$ , the maximum velocity (PGV) -  $0.649\text{ cm/s}$ , and the maximum displacement (PGD)  $0.0442\text{ cm}$ . The duration of the earthquake was  $t_D = 2.56\text{ s}$ . Soil oscillation recording was performed every  $0.0012\text{ s}$  (Zembaty 2004). Time series of 4050 data (north-south direction), 3600 data (east-west direction) and 2750 data (vertical direction) were used for the analysis. Figure 1 shows the time series of ground acceleration in three directions. The analysis was performed only for soil acceleration components, since the maximum soil acceleration is one of the main parameters included in the calculation of

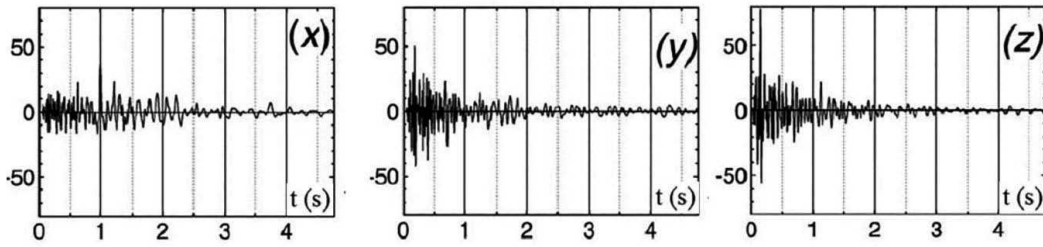


Figure 1. Time series of ground acceleration during the mining induced seismic event  $M \approx 2$  registered on 2<sup>nd</sup> February 2001 at Rudna mine in western Poland, at the 3 Maja station, in three directions: (x) - north-south; (y) - east west and (z) - vertically (Zembaty 2004).

building structures (Boore & Bommer 2005). Also, although accelerations in the horizontal direction are most often taken into account, due to their natural connection with inertial forces, an analysis of all three components of acceleration will be performed here, in order to examine the dynamic behavior of the soil during earthquakes in all three directions.

The test results of the first hypothesis (that the time series is composed of randomly selected numbers, without correlation with each other), where the surrogate data series were obtained by generating randomly selected initial data series, are shown in Figure 2(a). It is clear that in all three observed cases, the null hypothesis  $H_0$  is rejected, since  $\varepsilon > \varepsilon_0$  for each  $n$  and for each examined series of surrogate data. In this case, 20 different sets of surrogate data were generated, using the phase randomization procedure. Unlike the previous case, the test results of hypothesis II (the recordings originate from a stationary linear stochastic process with Gaussian inputs) indicate that  $\varepsilon \geq \varepsilon_0$  for the north-south direction and the vertical direction, while  $\varepsilon < \varepsilon_0$  for the registered accelerations of ground acceleration in the east-west direction, so it can be concluded that zero hypothesis  $H_0$  cannot be rejected for the case of registered ground acceleration in the east-west direction (Figure 2c).

The last step in the analysis of surrogate data is to test the hypothesis that the time series originates from a stationary Gaussian linear process, which is modified by an unknown nonlinear function. As in the previous case, 20 surrogates were generated for each direction of ground acceleration, using the “common” and iterative test procedure of surrogate data sets with

“tuned” amplitude (AAFT and IAAFT), and the prediction error  $\varepsilon$  was determined. The results of hypothesis III testing indicate that only in the case of ground acceleration in the east-west direction (Figure 3) we cannot reject the null hypothesis ( $\varepsilon < \varepsilon_0$ ). In all other cases, it is necessary to perform a correlation test, on the basis of which the null hypothesis would be accepted or rejected. Accordingly, it can be said that the ground acceleration in the north-south direction cannot be classified as a class of time series originating from a stationary Gaussian linear process, which is modified by an unknown nonlinear function.

Based on the previously performed analysis of surrogate data, it is clear that the components of ground acceleration in the north-south and vertical direction during mining-generated earthquakes are an example of nonlinear systems (all three null hypotheses were rejected after testing), while soil oscillations in the east-west direction belongs to the group of stochastic processes with Gaussian distribution of the stochastic work, which are modified by a nonlinear unknown function. Accordingly, in the case of ground acceleration in the east-west direction, nonlinear dynamic phenomena cannot be expected, primarily deterministic chaotic behavior. However, the analysis of nonlinear time series can be applied in this case as well. Namely, the application of these methods and techniques for a non-trivial case can give further confirmation of the correctness of the conducted analysis of surrogate data.

The first step in the analysis of nonlinear time series is to determine the optimal time interval of

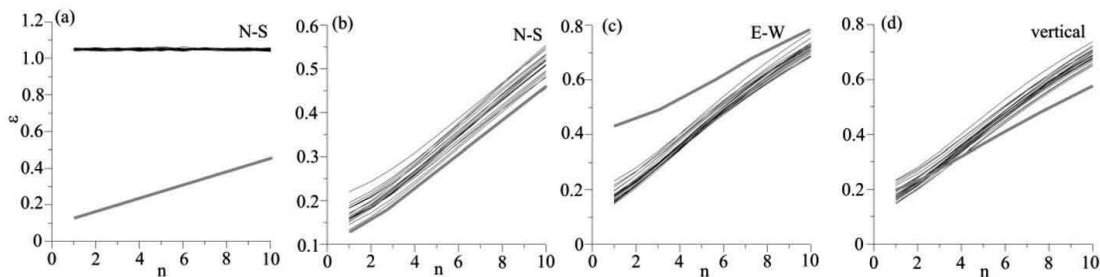


Figure 2. (a) Surrogate data testing of the first null hypothesis; qualitatively the same are obtained for other two directions; (b)-(d) surrogate data testing of the second null hypothesis. The gray line indicates the prediction error for the original time series ( $\varepsilon_0$ ), while the black lines indicate the error distribution for the surrogate data series ( $\varepsilon$ ).

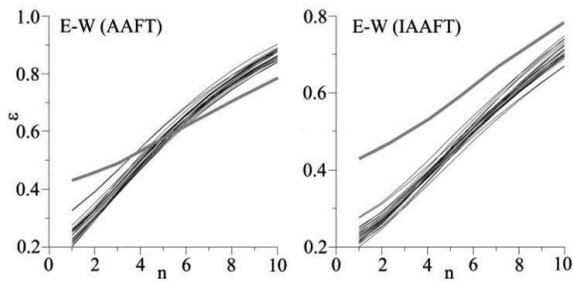


Figure 3. Hypothesis III testing of the recorded ground acceleration in east-west direction. The left column presents the results of the test with AAF procedure, the right column - the iterative procedure of testing the surrogate data series with “adjusted” amplitude (AAF and IAAFT). The gray line indicates the prediction error for the original time series ( $\epsilon_0$ ), while the black lines indicate the error distribution for the surrogate data sets ( $\epsilon$ ).

embedding. Using the mutual information method, the optimal value of the embedding delay for all three components of ground acceleration was determined, and the results are shown in Figure 4. Further we determine the minimum embedding dimension  $m$ , which is required for a complete reconstruction of the system attractor (if any). For the calculation, we use the previously defined technique of false nearest neighbour. Based on the results presented in Figure 4, it is clear that for all three directions of ground acceleration, the percentage of seemingly closest neighbouring values increases with increasing dimension of development, very quickly reaching peak values.

The next step of the analysis involves performing a stationarity test. In this case, the method of stationarity testing using the stationarity test (Perc et al. 2008) was adopted, which is based on the calculation of the mean square error of the future values of the environment of the selected point. The registered time series for all three soil acceleration components are divided by the same number of segments ( $41 \times 41$ ), but with a different number of data within each segment (since the number of data for the initial time series also differs). The stationarity test was performed for the value of the optimal dimension of development  $m = 5$ . Qualitatively similar results are

obtained for other values of the embedding dimension, in the interval  $m = 2-10$ . The results of the stationarity test for the north-south direction are shown in Figure 3(c). The color of each segment indicates an error in the prediction, using the value of the segment and to predict the value of the segment  $j$ . It is clear that for by far the largest number of pairs of segments there is a small to medium error in prediction, confirming the stationary nature of the examined process (“in the background”). The results of the east-west stationarity test show an “accumulation” of error for small sets of segments. Namely, the values of all segments do not give an accurate prediction of the values of the segment  $j = 1-7$ . The results of the stationarity test for the vertical direction, in contrast to the diagrams in the previous two cases,  $r$  show a very small percentage of high prediction error.

The next step in the analysis involves performing a deterministic test, which allows checking the deterministic nature of the process whose activity during a certain time interval is represented by the examined time series. In this case, to conduct a deterministic test, we reconstructed the vector field of the solution of the assumed system of differential equations of the original system, and then calculated the deterministic factor  $\kappa$ . For the purpose of performing the deterministic test, the previously reconstructed (embedded) phase space is divided by a grid of quadrants measuring  $41 \times 41 \times 41$  (which represents the maximum number of fields). In order to determine the deterministic factor  $\kappa$ , only those quadrants covered by the reconstructed vector field (through which the trajectories-solutions of the system pass) were taken into account. Since the value of the optimal dimension of embedding could not be determined using the test of the false nearest neighbour technique, the deterministic test was performed for several values of the embedding dimensions, in the interval  $m = 2-10$ . From Figure 4 it is clear that  $\kappa < 1$  (and does not converge to 1), indicating non-deterministic system dynamics.

After conducting a deterministic test, the value of the largest Lyapunov exponent was calculated using the method of determination, better known as Wolf’s method (Perc 2005), which is based on estimating

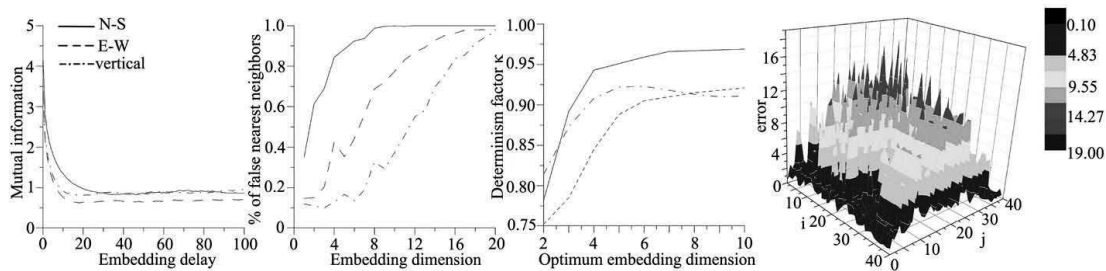


Figure 4. (a) Determining the optimal embedding delay for the registered ground acceleration. The mutual information function reaches the first minimum for  $\tau = 29$ ,  $\tau = 18$  and  $\tau = 12$ ; (b) Determination of the minimum value of embedding dimension  $m$  for the registered accelerations; (c) Change in the value of the deterministic factor  $\kappa$  for different values of the embedding dimension, for registered accelerations in different directions. The diagram shows the average error in cross-prediction  $\delta_{ij}$  depending on different combinations of segments.

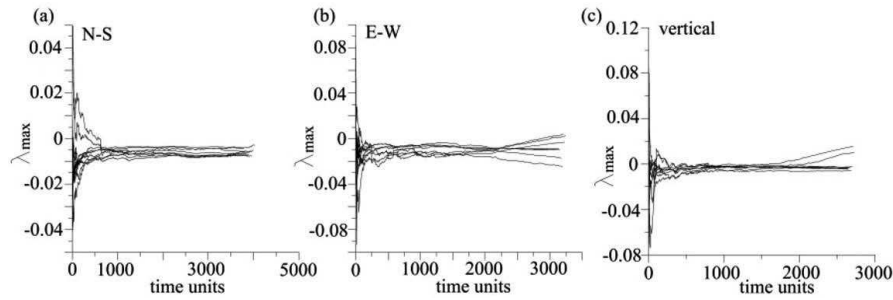


Figure 5. Largest Lyapunov exponent for different embedding dimensions  $m = 2-10$ , for registered time series of ground acceleration.

the change in the distance between the two closest values ( $L_0$ ), for a fixed time of system development ( $t_{\text{evolve}}$ ). Since the value of the optimal dimension of development was not determined by the method of the seemingly closest value, the determination of the maximum Lyapunov exponent for the dimensions of development in the interval  $m = 2-10$  was started (Figure 5). As can be seen, in all observed cases, the maximum Lyapunov exponent weighs a negative value, or a slightly positive value (for two values of the development dimension in soil oscillations in the east-west direction and in the vertical direction).

## 5 CONCLUSION

In present paper we analyze the ground acceleration induced by the seismic event  $M \approx 2$  registered on 2nd February 2001 at Rudna mine in western Poland. The analysis was done using the nonlinear time series analysis. It was shown that recorded time series belong to group of non-deterministic processes, with low determinism factor, clear non-stationarity and low value of maximal Lyapunov exponent. In particular, analyzed time series were firstly examined using surrogate data testing. The results of testing the dynamics of soil oscillations during mining-generated earthquakes indicated the nonlinear nature of the registered series, both north-south and vertical, while soil oscillations in the east-west direction belong to the class of stochastic processes with Gaussian distribution of stochastic part, which can be modified by some unknown nonlinear function. However, despite the fact that soil oscillations in the north-south and east-west directions belong to the group of nonlinear processes, the analysis of nonlinear time series showed that in these directions the soil oscillations also belong to stochastic processes. These results were confirmed by a low value of the deterministic factor  $\kappa$  ( $< 1$ ) and a low cross-prediction error in the stationarity test. Also, false nearest neighbour method did not give results in terms of determining the optimal embedding dimension, which again

indicates the stochastic nature of the registered ground acceleration.

Further research could include analysis of the ground acceleration triggered by stronger seismic event, in order to analyze whether the magnitude and intensity of the mining-induced earthquake have any impact on the qualitative properties of ground acceleration.

## REFERENCES

- Huang, G., Yin, G., Dai, G. 2010. Chaotic behavior of a stick-slip model for rockburst. *Disaster Advances* 3: 526–530.
- Kortas, L. 2005. Search for chaotic dynamics manifestation in multiscale seismicity, *Acta Geophysica Polonica* 53: 47–74.
- Kwiatek, G. & Debski, W. 2006. Source tomography of mining-induced seismic events at “Rudna” and “Polkowice-Sieroszowice” copper mine. *First European Conference on Earthquake engineering and seismology*, Geneva, Switzerland.
- Morrison, D. M., Swan, G., Scholz, C. H. 1993. Chaotic behavior and mining-induced seismicity, In: Young, R.P. (ed.) *Rockbursts and Seismicity in Mines*, Balkema, Rotterdam, 233–237.
- Oszczepalski S. 1989. Kupferschiefer in southwestern Poland. Sedimentary environment, metal zoning, and ore controls. In: Sediment hosted copper deposits, Boyle, R.W., Brown, A.C., Jefferson, C.W., Jowett, E.C., Kirkham, R.V. (eds). *Canadian Special Papers*, Waterloo, Ontario, 571–600.
- Perc, M. 2005. Nonlinear time series analysis of the human electrocardiogram. *Eur. J. Phys.* 26: 757–768.
- Perc, M., Green, A.K., Jane Dixon, C., Marhl, M. 2008. Establishing the stochastic nature of intracellular calcium oscillations from experimental data, *Biophysical Chemistry* 132: 33–38.
- Takens, F. 1981. Detecting strange attractors in turbulence. In D. A. Rand and L.-S. Young. *Dynamical Systems and Turbulence, Lecture Notes in Mathematics*, Springer-Verlag 898: 366–381.
- Zembaty, Z. 2004. Rockburst induced ground motion – a comparative study. *Soil Dynamics and Earthquake engineering* 24: 11–23.